EMBEDDED NDE WITH PIEZOELECTRIC WAFER-ACTIVE SENSORS IN AEROSPACE APPLICATIO

Abstract:

The capability of embedded piezoelectric wafer-active sensors (PWAS) to perform in-situ nondestructive evaluation (NDE) is explored in this article, which includes animations of PWAS interactions with Lamb modes. PWAS can satisfactorily perform Lamb wave transmission and reception, and crack detection in an aircraft panel with the pulse-echo method is illustrated. For large-area scanning, a PWAS phased array is used to create the embedded ultrasonic structural radar. For quality assurance, PWAS are self-tested using electromechanical impedance.
Embedded nondestructive evaluation (NDE) is an emerging technology that will allow for the transitioning from conventional ultrasonic methods to embedded systems structural health monitoring (SHM), such as those envisioned for the Integrated Vehicle Health Management (IVHM). Structural health monitoring for IVHM requires the development of small, lightweight, inexpensive, unobtrusive, minimally invasive sensors to be embedded in the airframe with minimum weight penalty and at affordable costs. Such sensors should be able to scan the structure and identify the presence of defects and incipient damage.

Introduction

Current ultrasonic inspection of thin-wall structures (e.g., aircraft shells, storage tanks, large pipes, etc.) is a time-consuming operation that requires meticulous through-the-thickness C-scans over large areas. One method to increase the efficiency of thin-wall structures inspection is to utilize guided waves (e.g., Lamb waves) instead of the conventional pressure waves. Guided waves propagate along the mid-surface of thin-wall plates and shallow shells. They can travel at relatively large distances with very little amplitude loss and offer the advantage of large-area coverage with a minimum of installed sensors. Guided Lamb waves have opened new opportunities for the cost-effective detection of damage in aircraft structure. Traditionally, guided waves have been generated by impinging the plate obliquely with a tone-burst from a relatively large ultrasonic

transducer. Snell's law ensures mode conversion at the interface, hence, a combination of pressure and shear waves are simultaneously generated into the thin plate. However, conventional Lamb-wave probes (wedge and comb transducers) are too heavy and expensive to be considered for widespread deployment on an aircraft structure as part of a SHM system. Therefore, a different type of sensors than the conventional ultrasonic transducers is required for the SHM systems.

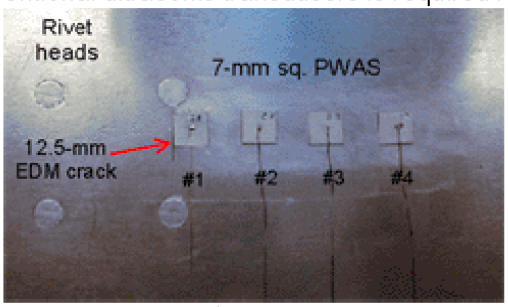

Figure 1. Piezoelectric wafer active sensors (PWAS) mounted on an aircraft panel.

Several investigators have recently explored the generation of Lamb-waves with piezoelectric wafer-active sensors (PWAS). Piezoelectric wafer-active sensors are inexpensive, non-intrusive, unobtrusive, and minimally invasive devices that can be surface-mounted on existing structures inserted between the layers of lap joints or inside composite materials. Figure 1 shows an array of 7 mm square PWAS mounted on an aircraft panel, adjacent to rivet heads and an electric-discharge machined (EDM) simulated crack. The minimally invasive nature of the PWAS devices is apparent. These PWAS weigh around 68 mg, are 0.2 mm thick, and cost $7. They operate on the piezoelectric principle that couples the electrical and mechanical variables in the material (mechanical strain, S_{ij}, mechanical stress, T_{kl}, electrical field, E_k, and electrical displacement D_j) in the form:

$$S_{ij} = s^{E}_{ijkl} T_{kl} + d_{kij} E_k$$
$$D_j = d_{jkl} T_{kl} + \varepsilon^{T}_{jk} E_k \ , \qquad (1)$$

where S^{E}_{ijkl} is the mechanical compliance of the material measured at zero electric field (E = 0), ε^{T}_{jk} is the dielectric permittivity measured at zero mechanical stress (T = 0), and d_{kij} represents the piezoelectric coupling effect. For embedded NDE applications, PWAS couple their in-plane motion, excited by the applied oscillatory voltage through the piezoelectric effect, with the Lamb-wave-particle motion on the material surface. Lamb waves can be either quasi-axial (S0, S1, S2, . . .) or quasi-flexural (A0, S1, S2, . . .). Piezoelectric wafer-active sensor probes can act as both exciters and sensors of the elastic Lamb waves traveling in the material.

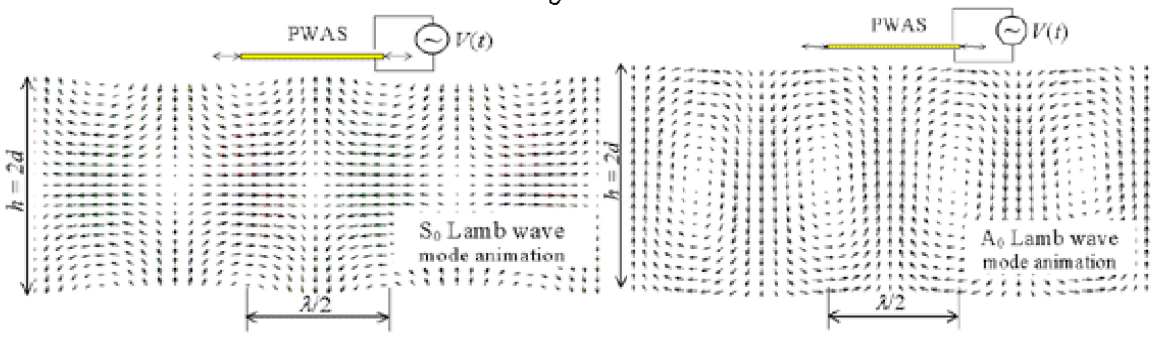

PWAS interaction with (a) S_0 and (b) A_0 Lamb modes.

For non-destructive evaluation, PWAS can be used as both active and passive probes. Thus, they address four IVHM-SHM needs:

- Far-field damage detection using pulse-echo and pitch-catch methods
- Near-field damage detection using a high-frequency impedance method
- Acoustic emission monitoring of crack initiation and growth
- Low-velocity impact detection

Piezoelectric wafer-active sensors operation is different than that of conventional ultrasonic probes. For example, PWAS achieve Lamb-wave excitation and sensing through surface "pinching" (in-plane strains), while conventional ultrasonic probes excite through surface "tapping" (normal stress). In addition, PWAS are strongly coupled with the structure and follow the structural dynamics, while conventional ultrasonic probes are relatively free from the structure and follow their own dynamics. Finally, PWAS are non-resonant wide-band devices, while conventional ultrasonic probes are narrow-band resonators.

The main advantage of PWAS over conventional ultrasonic probes lies in their small size, light weight, low profile, and low cost. In spite of their size, these novel devices are able to replicate many of the functions of the conventional ultrasonic probes, as proven by the proof-of-concept laboratory demonstrations described.

PWAS-GENERATED LAMB WAVES

The basic principles of Lamb-wave generation and detection by PWAS probes were first verified in simple laboratory experiments. A 1.6-mm-thick, 2024-aluminum alloy rectangular plate (914 mm × 504 mm × 1.6 mm) was instrumented with 11 7-mm-square, 0.2-mm thick PWAS that were placed on a rectangular grid. Omnidirectional transmission is achieved and signals are strong enough and attenuation is sufficiently low for echoes to be detected. The proof of these attributes is especially important for PWAS, which are at least an order of magnitude smaller and lighter than conventional ultrasonic transducers.

To prove that the Lamb waves excited by PWAS are omnidirectional, one PWAS (11) was used as a transmitter and the other PWAS (1–10) as receivers. The signals observed in this investigation are shown in Figure 2a. In each row, the electromagnetic coupling of the initial bang is shown around the origin. Then, the first wave package corresponding to the wave received from the transmitter PWAS is seen, followed by other wave packages corresponding to reflections from the plate edges. The time difference between the initial bang and the wave-package arrival represents the time-of-flight (TOF). The TOF is consistent with the distance traveled by the wave. Figure 2b shows the straight-line correlation between TOF and distance. The slope of this line is the experimental group velocity, c_g = 5.446 km/s, while the theoretical value should be 5.440 km/s. Very good accuracy is observed (99.99% correlation; 0.1% speed detection error), proving that PWAS-generated Lamb waves are loud and clear, propagate omnidirectionally, and correlate well with the theory.

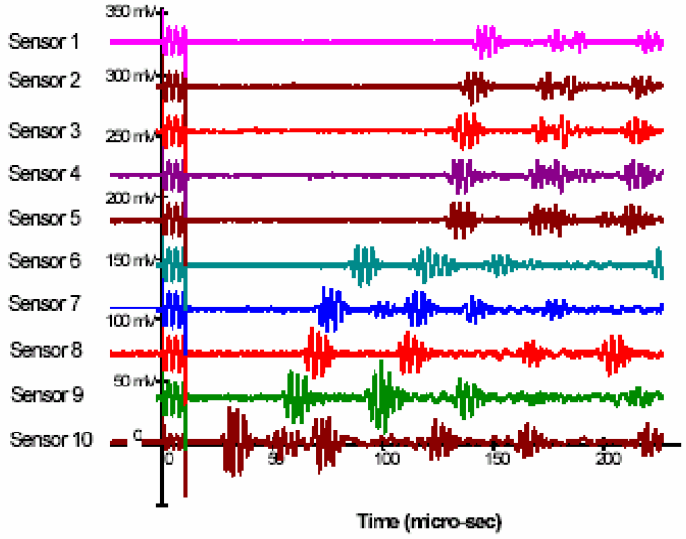

(a)

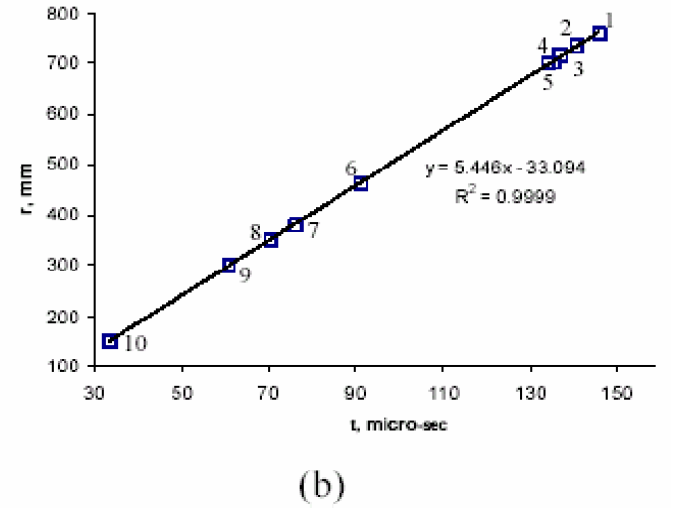

(b)

Figure 2. (a) Reception signals on active sensors one through ten; (b) the correlation between radial distance and time of flight

PULSE-ECHO WITH PWAS

Piezoelectric wafer-active sensor 11 was used to demonstrate pulse-echo capabilities. Figure 3a shows that the sensor 11 signal has two distinct zones: the initial bang, during which the PWAS 11 acts as transmitter, and the echoes zone, containing wave packs reflected by the plate boundaries and sent back to PWAS 11. These echoes were processed to evaluate the pulse-echo capabilities of the method. Since the wave generated by the initial bang underwent multiple reflections from the plate edges, each of these reflections had a different path length, as shown in Figure 3b. It is interesting to note that the path lengths for reflections R_1 and R_2 are approximately equal. Hence, the echoes R_1 and R_2 in the pulse-echo signal of Figure 3a are almost superposed.

Also interesting to note is that the reflection R_4 has two possible paths, R_{4a} and R_{4b}, of the same length. Hence, the echoes corresponding to these two reflection paths arrive simultaneously and form a single but stronger echo signal, which has roughly twice the intensity of the other echoes. A

plot of the TOF of each echo vs. its path length is given in Figure 3c. The straight-line fit has a very good correlation (R^2 = 99.99%). The corresponding wave speed is 5.389 km/s (i.e., within 1% of the theoretical value of 5.440 km/s). The echoes were recorded from over 2 m distance, which is remarkable for such small ultrasonic devices. Thus, it was proven that the PWAS are fully capable of transmitting and receiving pulse-echo signals of remarkable strength and clarity.

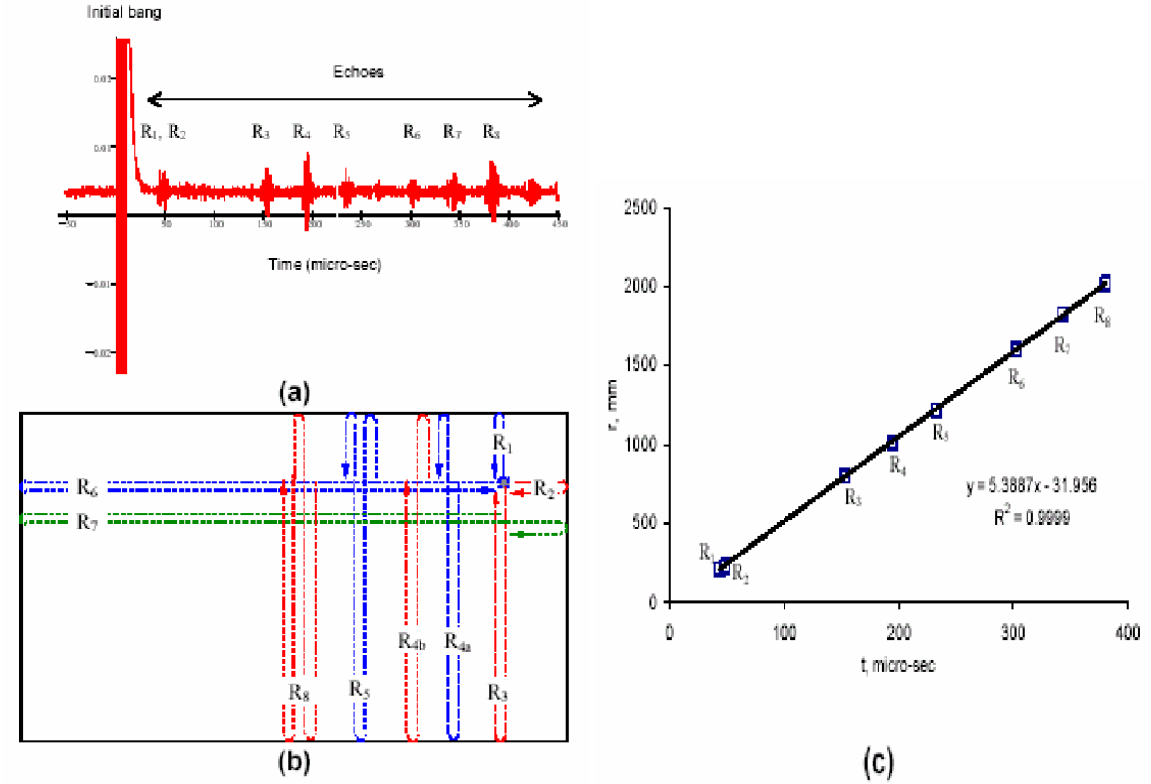

Figure 3. The pulse-echo method applied to active sensor 11: (a) the excitation signal and the echo signals on active sensor 11, (b) a schematic of the wave paths for each wave pack, and (c) correlation of path length with time of flight.

PWAS CRACK DETECTION

Wave-propagation experiments were conducted on an aircraft panel to illustrate crack detection through the pulse-echo method. The panel has a typical aircraft construction, featuring a vertical splice joint and horizontal stiffeners. Figures 4a,4b and 4c show three photographs of PWAS installation on increasingly more complex structural regions of the panel. Figures 4d, 4e, 4f and 4g show the PWAS signals. All the experiments used only one PWAS, operated in pulse-echo mode. The PWAS was placed in the same relative location (i.e., at 200 mm to the right of the vertical row of rivets). Figure 4a shows the situation with the lowest complexity, in which only the vertical row of rivets is present in the far left. Figure 4d shows the initial bang (centered at around 5.3 microseconds) and multiple reflections from the panel edges and the splice joint. The echoes start to arrive at approximately 60 micrometer. Figure 4b shows the vertical row of rivets in the far left and, in addition, a horizontal double row of rivets stretching toward the PWAS. Figure 4e shows that, in addition to the multiple echoes from the panel edges and the splice, the PWAS also receives backscatter echoes from the rivets located at the beginning of the horizontal row. These backscatter echoes are visible at around 42 micrometer. Figure 4c shows a region of the panel

similar to that presented in the previous row, but having an additional feature: a simulated crack (12.7 mm EDM hairline slit) emanating from the first rivet hole in the top horizontal row. Figure 4g shows features similar to those of the previous signal, but somehow stronger at the 42 micrometer position. The features at 42 micrometer correspond to the superposed reflections from the rivets and from the crack. The detection of the crack seems particularly difficult because the echoes from the crack and from the rivets are superposed.

This difficulty was resolved by using the differential signal method (i.e., subtracting the signal presented in Figure 4e from the signal presented in Figure 4f). In practice, such a situation would correspond to subtracting a signal previously recorded on the undamaged structure from the signal recorded now on the damaged structure. Such a situation of using archived signals is typical of health monitoring systems. When the two signals were subtracted, the result presented in Figure 4g was obtained. This differential signal shows a loud and clear echo due entirely to the crack. The echo, marked "reflection from the crack" is centered at 42 micrometer (i.e., TOF = 37 micrometer) which correlates very well with a 5.4 km/s 200 mm total travel from the PWAS to the crack placed at 100 mm. The cleanness of the crack-detection feature and the quietness of the signal ahead of the crack-detection feature are remarkable. Thus, PWAS were determined to be capable of clean and unambiguous detection of structural cracks. A manual sweep of the beam angle can be also performed with the turn knob; the signal reconstructed at the particular beam angle (here, θ_0 = 136°) is shown in the lower picture.

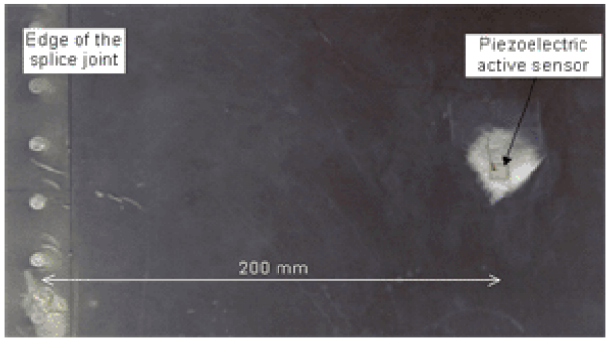

A

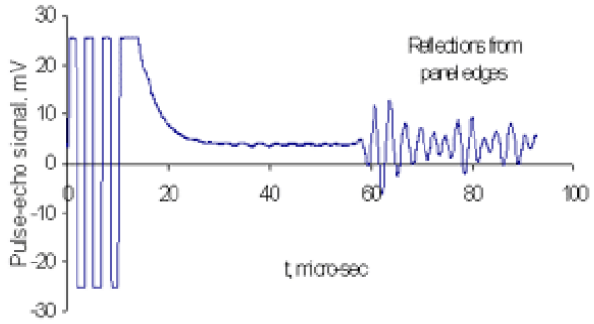

d

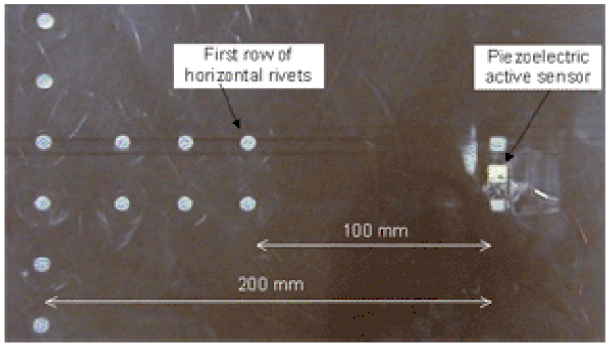

B

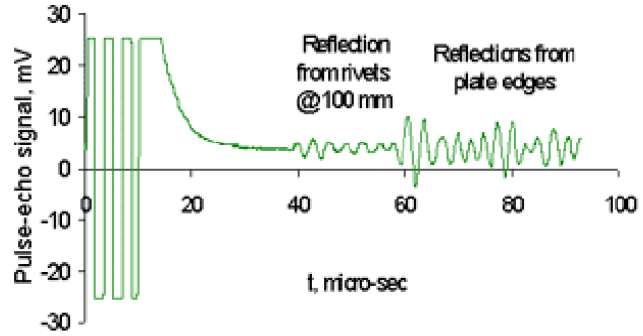

e

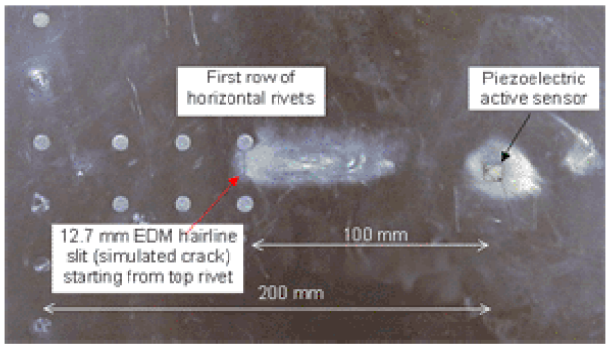

c

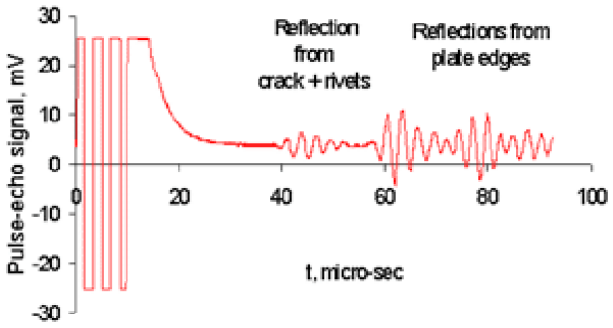

f

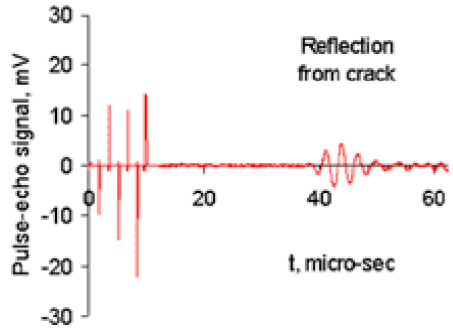

g

Figure 4. Crack-detection laboratory experiments on an aircraft panel: 4a-4c are specimens (1 mm 2025 T3) with increasing complexity. 4d-4g represent the pulse-echo signals; 4g shows the crack detection through the differential signal method.

PWAS PHASED ARRAYS

The advantages of phased-array transducers for ultrasonic testing are multiple. Krautkramer, Inc. produces a line of phased-array transducers for the inspection of very thick specimens and for the sidewise inspection of thick slabs, etc. These transducers employ pressure waves generated through normal impingement on the material surface. In this a phased-array technology was developed for thin-wall structures (e.g., aircraft shells, storage tanks, large pipes, etc.) that uses Lamb waves to cover a large surface area through beam steering from a central location. This concept is called as embedded ultrasonics structural radar (EUSR). A PWAS array was made up of a number of identical 7 mm square elements aligned at uniform 9 mm pitch. The PWAS phased array was placed at the center of a 1.2 m square thin aluminum plate (Figure 5). The wave pattern generated by the phased array is the result of the superposition of the waves generated by each individual element. By sequentially firing the individual elements of an array transducer at slightly different times, the ultrasonic wave front can be focused or steered in a specific direction. Thus, electronic sweeping and/or refocusing of the beam was achieved without physically manipulating the transducers. In addition, inspection of a wide zone was possible by creating a sweeping beam of ultrasonic Lamb waves covering the whole plate. Once the beam steering and focusing was established, crack detection was done with the pulse-echo method. During these proof-of-concept experiments, the EUSR methodology was used to detect cracks in two typical situations: a 19-mm broadside crack placed at 305 mm from the array in the 90° direction, and a 19 mm broadside crack placed 409 mm from the array in the 136° direction. Of these two, the latter was more challenging because the ultrasonic beam is not reflected back to the source but rather deflected sideways. Hence, the echo received from the offside crack is merely the backscatter signal generated at the crack tips. The sweep is performed automatically to produce the structural defect image in the right pane. Manual sweep can be performed with the turn knob. The lower pane shows the signal reconstructed at the beam angle θ_0 = 136° corresponding to the crack location.

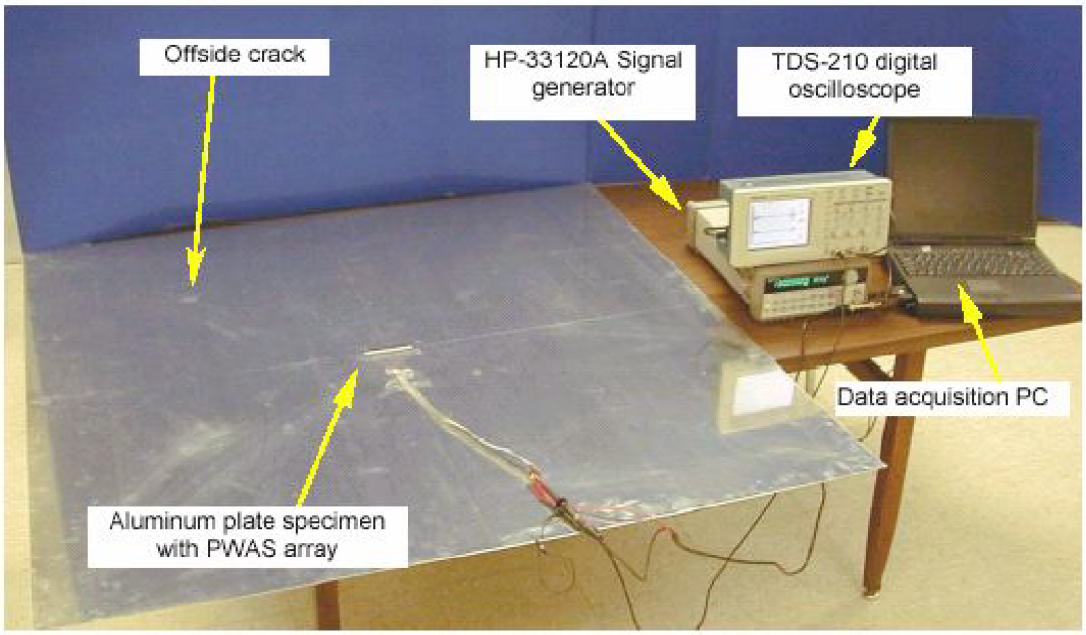

(a)

Figure 5 – Proof-of-concept EUSR experiment: (a) thin plate specimen 9-element PWAS array and 19-mm offside crack; (b) Graphical user interface (EUSR-GUI) front panel. The angle sweep is performed automatically to produce the structure/defect imaging picture on the right. Manual sweep of the beam angle can be also performed with the turn knob; the signal reconstructed at the particular beam angle (here, ö0 = 136 deg) is shown in the lower picture.

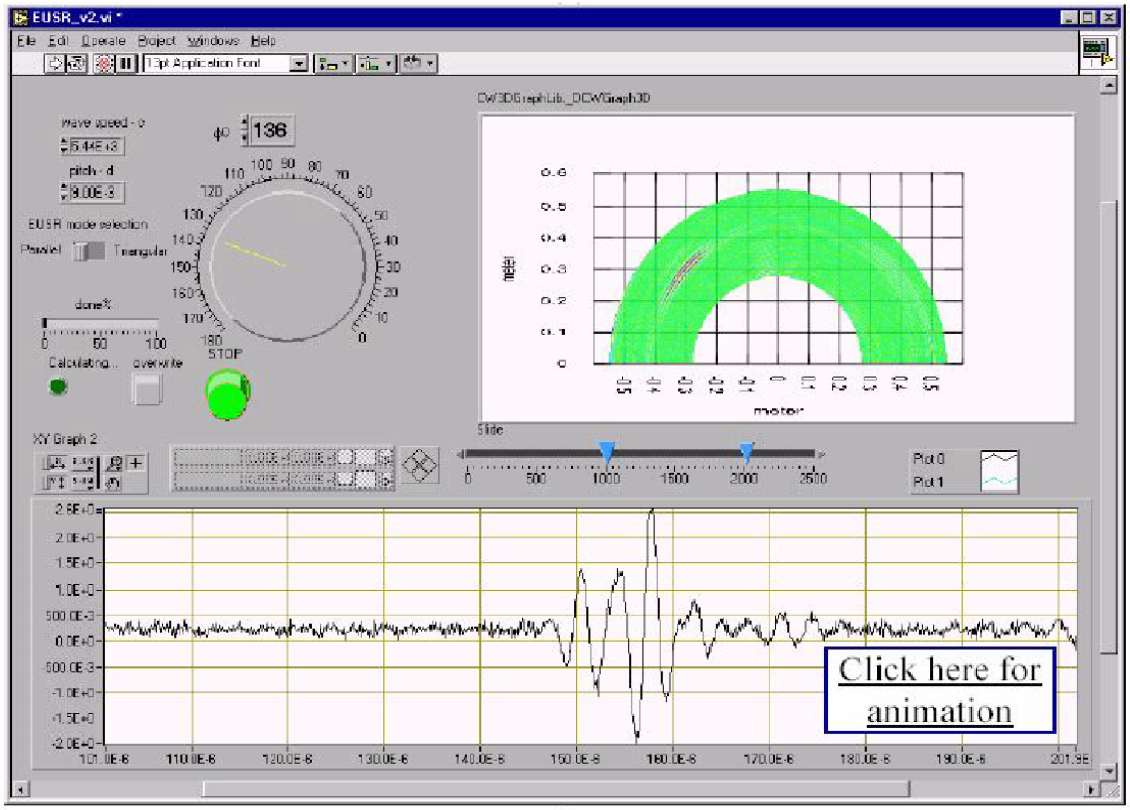

(b)

fig 5b

PWAS SELF-TEST

Since the PWAS probes are adhesively bonded to the structure, the bond durability and the possibility of the probe becoming detached are of concern. To address this, a PWAS self-test procedure has been identified that can reliably determine if the sensor is still perfectly attached to the structure. The procedure is based on PWAS in-situ electromechanical impedance.

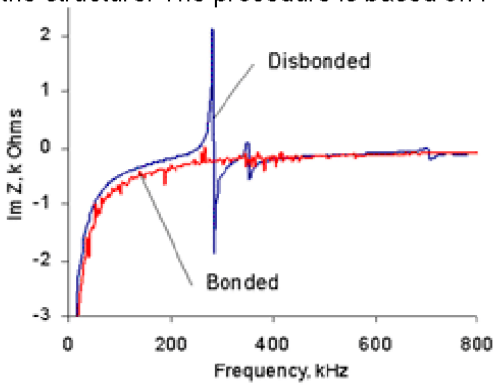

Figure 6. A PWAS self test: when sensor is disbonded, a clear free-vibration resonance appears at ~267 kHz.

Figure 6 compares the Im Z spectrum of a well-bonded PWAS with that of a disbonded (free) PWAS. The well-bonded PWAS presents a smooth Im Z curve, modulated by small structural resonances. The disbonded PWAS shows a strong self-resonance and no structural resonances. The appearance of the PWAS resonance and the disappearance of structural resonances constitute features that can unambiguously discern when the PWAS has become disbonded and

can be used for an automated PWAS self-test. For a partially disbonded PWAS, a mixture of PWAS and structure vibration was recorded.

Conclusion

Embedded NDE piezoelectric wafer active s can be structurally embedded as both individual probes and phased arrays. They can be placed even inside closed cavities during fabrication/overhaul (such as wing structures), and then be left in place for the life of the structure. The embedded NDE concept opens new horizons for performing in-situ damage detection and structural health monitoring of a multitude of thin-wall structures such as aircraft, missiles, pressure vessels, etc.

Address for Communication :

NAME : D. LAKSHMA REDDY (Final year E.I.E)
GROUP: B.TECH (E.I.E)
DEPT : Electronics & Instrumentation Engineering

Address :-

D.LAKSHMA REDDY
C/o SHRIDI SAI SADHAN
D.No :: 8-1-10
BHIMAVARIPALEM
BAPATLA-522101
e-mail: mlakshma20@yahoo.co.in